Research Article • DOI: 10.2478/kinome-2013-0001 • KINOME • 2013 • 4–16

An atypical cyclin-dependent kinase controls *Plasmodium falciparum* proliferation rate

Abstract

Malaria parasites multiply in human erythrocytes through schizogony, a process characterised by nuclear divisions in the absence of cytokinesis, leading to the formation of a multinucleated schizont from which individual daughter cells are subsequently generated. Here, we provide evidence that parasites lines lacking Pfcrk-5, an atypical cyclin-dependent kinase, display a reduced parasitemia growth rate linked to a decrease in the number of daughter nuclei produced by each schizont. We show that *in vitro* activity of recombinant Pfcrk-5 is indeed cyclin-dependent, and that the enzyme localises to the nuclear periphery. Thus, Pfcrk-5 is part of a regulatory pathway that mediates the proliferation rate of *Plasmodium falciparum* through the control of nuclear divisions during schizogony.

Keywords

Cyclin-dependent kinase • *Plasmodium falciparum* • Pfcrk-5 • Cell cycle • Malaria

Dominique Dorin-Semblat[1,2,+], Teresa Gil Carvalho[3], Marie-Paule Nivez[2], Jean Halbert[1,2], Patrick Poullet[4], Jean-Philippe Semblat[1,2,+], Dean Goldring[5], Debopam Chakrabarti[6], Parul Mehra[7], Suman Dhar[7], May M.Paing[8], Daniel E. Goldberg[8], Paul J. McMillan[9,10], Leann Tilley[9,10], Christian Doerig[1,2,3*]

[1]INSERM-EPFL Joint Laboratory, Global Health Institute, Ecole Polytechnique Fédérale de Lausanne, GHI-SV-EPFL Station 19, CH-1015 Lausanne, Switzerland

[2]INSERM U609, Wellcome Centre for Molecular Parasitology, University of Glasgow, Glasgow G12 8TA, Scotland, UK

[3]Department of Microbiology, Monash University, Wellington Road, Clayton, VIC 3800, Australia.

[4]Institut Curie, 26 Rue d'Ulm, 75248 PARIS cedex 05, France

[5]Biochemistry, University of Kwazulu-Natal, PB X01 Scottsville, South Africa

[6]Dept. of Molecular Biology and Microbiology, University of Central Florida, 12722 Research Parkway Orlando FL32826, USA

[7]Special Centre for Molecular Medicine, Jawaharlal Nehru University, New Delhi-110067, India

[8]Departments of Medicine and Molecular Microbiology, Howard Hughes Medical Institute, Washington University Box 8230, 660 S. Euclid Ave, St. Louis, MO 63110, USA

[9]Department of Biochemistry and Molecular Biology, Bio21 Molecular Science and Biotechnology Institute, The University of Melbourne, Parkville, 3010, Victoria, Australia

[10]Australian Research Council Centre of Excellence for Coherent X-ray Science, The University of Melbourne, Parkville, 3010, Victoria, Australia

[+]Present address: Inserm U665, Institut National de Transfusion sanguine, 6, rue Alexandre Cabanel, 75739 Paris Cedex 5, France

Received 24 January 2013
Accepted 24 February 2013

INTRODUCTION

Malaria parasites are apicomplexan protists of the genus *Plasmodium*, five species of which infect humans. Their life cycle is complex and involves shuttling between the human host and an *Anopheles* mosquito vector. *Plasmodium* sporozoites are injected into the host by the insect during a blood meal and gain the liver, where a first round of schizogony occurs, producing merozoites that are geared to invade erythrocytes. Asexual proliferation by schizogony in the red blood cell is the phase of the life cycle that is responsible for malaria pathogenesis. The parasite is transferred back to the mosquito through male and female gametocytes, which are cell cycle-arrested, sexually differentiated cells that develop in a fraction of the invaded erythrocytes. Upon ingestion by the insect, the gametocytes complete their development into gametes, and the endpoint of the sexual cycle in the mosquito is the accumulation of sporozoites in the mosquito's salivary glands, where they are primed for infection of a new human host.

Despite a significant decrease in global mortality caused by malaria in recent years, which was in part brought about by the introduction of arteminisin-based combination therapies (ACT), this disease still takes almost a million lives every year, and significantly impairs socio-economic development in many parts of the developing world [1]. In view of the worrying emergence of decreased susceptibility to ACT in *Plasmodium falciparum*, the species responsible for the most virulent form of human malaria, developing novel chemotherapeutic agents remains an urgent task [1,2]. The central role played by protein phosphorylation in essentially all complex processes in eukaryotic cells, and the success in targeting eukaryotic protein kinases (ePKs) in cancer chemotherapy [3], point to the divergent protein kinases of malaria parasites as potentially attractive, druggable targets for novel antimalarials with new modes of action [4,5]. The parasite's kinome comprises

* *E-mail: christian.doerig@monash.edu*

85-99 enzymes, depending on the stringency for inclusion applied to borderline sequences [6-8]. If one excludes the FIKKs, a novel, apicomplexan-specific family of 20 ePK-like sequences [6,9], the most numerous kinase group in the parasite's kinome is the 18-member strong CMGC group (CDK, MAPK, GSK and CDK-like), which in other eukaryotes comprises enzymes playing central roles in the control of cell proliferation and development.

The cyclin-dependent kinases (CDKs) constitute a large ubiquitous family of ePKs fulfilling regulatory functions [10], and which are the targets of numerous drug discovery initiatives (reviewed in [11-13]). Mammalian CDK1-4 and CDK6 control cell cycle progression, while CDK5 is involved in neuronal functions [14]. CDK8-11 regulate gene expression through a variety of effectors, including RNA polymerase II, other transcriptional proteins and the mRNA splicing machinery [15-18]. CDK7 plays crucial roles in both cell cycle control and transcription, notably through its CDK-activating kinase (CAK) activity, through which it phosphorylates other CDKs in their activation loop [19]. The activity of CDKs is regulated in a number of ways, including activation by cyclin binding, inhibitory or stimulatory phosphorylation / dephosphorylation by specific kinases (including CAKs) and phosphatases, and inhibition by polypeptidic inhibitors (CKIs). The 18 *P. falciparum* CMGC kinases include six enzymes that are more related to CDKs than to other families in the CMGC group [6,20]. Demonstration of cyclin-dependence has been provided for two of those, PfPK5 [21] and Pfmrk [22], the putative homologues of CDK1 and CDK7, repsectively, and we previously identified four genes encoding cyclin-related proteins in the parasite's genome [21,23]. Biochemical characterization has been published for five of the parasite's six CDK-related kinases: PfPK5 is the only plasmodial enzyme that clusters with the mammalian cell cycle CDKs, while Pfcrk-1 and Pfcrk-3 cluster with the transcriptional CDKs [24]; in line with these phylogenetic observations, Pfcrk-3 has been shown to interact with chromatin modification enzymes [24]. As mentioned above, Pfmrk was identified as a putative CDK7 homologue [25]. In addition to these four classical-looking CDKs, the *P. falciparum* CMGC group includes a branch comprising two unique sequences that are clearly related to CDKs but have no orthologues in the mammalian kinome. These are PfPK6, a kinase that displays cyclin-independent activity *in vitro* [26], and an as yet uncharacterized atypical enzyme, Pfcrk-5 (PlasmoDB accession number PFF0750w / PF3D7_0615500). We showed in a recent kinome-wide reverse genetics analysis that parasite lacking Pfcrk-5 are viable, but display a decreased rate of proliferation in human erythrocytes [27]. This is similar to the phenotype we observed in parasites deficient in another kinase, the atypical enzyme PfPK7 [28]. The slow proliferation rate of *pfpk7*$^{-}$ parasites is linked, not to a longer schizogonic cycle, but to a decreased number of daughter merozoites generated per schizont, implicating PfPK7 in the control of the unusual cell cycle exhibited by *Plasmodium* erythrocytic schizogony [28].

The cell cycle organization during this phenomenon (reviewed in [29,30]) is indeed widely divergent from that in model eukaryotes such as yeast or mammalian cells. The invading merozoite is thought to be in G0, and the early stage of development immediately following invasion of the RBC (the so-called ring stage) corresponds to the G1 phase of the cell cycle. S phase is initiated at the trophozoite stage, around 18 hours post invasion. Thereafter, nuclear divisions occur in the absence of cytokinesis, resulting in a multinucleated schizont. Interestingly, these nuclear divisions occur asynchronously, as demonstrated by the presence of mitotic spindles at various stages of development in the same schizont, and by a distribution of nuclei numbers per schizont that is incompatible with synchronous divisions [31,32]. This was recently confirmed by the observation that at any given time, only a subset of nuclei in a given schizont display association of an Aurora-related kinase with the spindle pole bodies, and are thus at a distinct phase of the division cycle [33].

Understanding the molecular basis for the slow growth phenotypes of PfPK7 and Pfcrk-5 would provide useful insights into cell cycle control in malaria parasites, and might reveal parasite-specific potential targets for intervention. Here, we demonstrate that Pfcrk-5 is indeed and cyclin-dependent kinase, and that is is located at the nuclear periphery. We show that the slow growth phenotype of *pfcrk-5*$^{-}$ parasites is caused by a lower average number of daughter merozoites produced by schizonts, exactly mimicking the PfPK7 phenotype. This paves the way for in-depth molecular studies of cell proliferation in malaria parasites.

EXPERIMENTAL PROCEDURES

Parasite culture and transfection

The 3D7 clone *of P. falciparum* was grown as described at 5% haematocrit in 5% CO_2 [34] and used for all experiments. Ring-stage parasites obtained by sorbitol treatment [35] were transfected with 100µg plasmid, and blasticidin selection (2.5 µg/ml) was applied from 2 days post transfection and maintained continuously. Gametocytogenesis induction was carried out as described by Carter *et al.* [36].

Molecular cloning of Pfcrk-5 and site-directed mutagenesis

The full-length Pfcrk-5 ORF (2118 bp) was amplified by PCR from a cDNA asexual library with Phusion Polymerase and cloned in the bacterial expression vector pGEX4T3 between the *Bam*H1 and *Sal*1 sites, using the following primers (restriction sites are underlined): Forward: 5'-GGGGGGATCCATGTTTGGAATTACATTAACAAAGTG-3'; Reverse: 5'-GGGGGTCGACTTAAAAATGAGAAAATTCTAGATGAC-3'. The construct was verified by DNA sequencing prior to bacterial expression in *E. coli*. A plasmid encoding a kinase-dead mutant enzyme (Lysine 38 to Methionine) was obtained by site directed mutagenesis using the overlap extension PCR technique [37] using the following primers containing the mutation: Forward: 5'-GTTTATGCCATAATGTTTTTTCGAGAC-3'; Reverse: 5'-GTCTCGAAAAAACATTATGGCATA-3'. The plasmid was sequenced to verify that no additional mutations had been generated during the PCR.

Generation of Pfcrk-5^{-} parasite by gene disruption

A 507 bp DNA fragment spanning nucleotides 88 to 795 of the Pfcrk-5 ORF was cloned into the pCAM-BSD vector carrying a blasticidin-resistance cassette [38] after PCR amplification from wild-type 3D7 genomic DNA using the following oligonucleotides: Forward: 5'-GGGGGGATCCACCTATGGTGACGTGTACAAAGGG-3'; Reverse: 5'-GGGGGCGGCCGCCAAAGGTCGGTAATATATTGTACAAAC-3', containing *Bam*H1 and *Not*1 restriction sites, respectively (underlined). Transfection was carried out as described above. Resistant parasites appeared after 4 weeks of blasticidin selection. After verifying by PCR that the desired genotype was well represented in the resistant population, the resistant parasites were cloned by limiting dilution in 96-well plates by seeding at 0.25, 0.5 and 1 parasite per well [39].

Expression and purification of GST-Pfrk-5 and cyclins

Pfcrk-5, Pfcyc-1, Pfcyc-2 and Pfcyc-4 [23] were purified as GST fusion proteins. Briefly, pGEX^{4T3} fusion constructs were used for protein expression in BL21 (DE3) codon plus cells in the presence of ampicillin (50 µg/ml) and chloramphenicol (25µg/ml). The cultures, at O.D. ~0.4, were induced with 0.5 mM IPTG and further incubated at 22°C for 6 hours. After induction, cells were harvested and the pellet was stored at –80°C. For the purification of recombinant protein, cells were further lysed at 4°C in lysis buffer (1xPBS, 10 mM DTT, 2 mM EDTA, 100 µM PMSF and 1 mg/ml lysozyme). The lysate was sonicated and incubated at 4°C with 0.1% Triton X-100 for 1 hour at 4°C. Supernatant was clarified by high-speed centrifugation. Soluble fraction of the protein was further incubated with pre-equilibrated Glutathione-sepharose 4B beads (Amersham) at 4°C for 1 hour. Unbound protein was separated by the centrifugation and protein bound beads were washed with lysis buffer containing 150 mM NaCl. Proteins were eluted with elution buffer containing 50mM Tris-HCl (pH 8.0), 10 mM DTT, 20 mM Glutathione, 0.1% NP-40, 10% Glycerol and 100 mM NaCl. Purified proteins were dialyzed and stored at -80°C.

Pfcyc-3 and Ringo were expressed as MBP fusion proteins. Briefly, pMAL$_{c2x}$ fusion constructs were expressed in BL21 (DE3) codon plus cells in the presence of ampicillin (50µg/ml) and chloramphenicol (25µg/ml). Induction conditions and harvesting were similar to the GST-fusion protein purification described above. Cells were re-suspended in lysis buffer containing 20 mM Tris-HCl (pH 8.0), 200 mM NaCl, 1 mM EDTA, 10 mM ß-mercaptoethanol, 100 µM PMSF and 1 mg/ml lysozyme. The lysate was sonicated and incubated at 4°C with 0.1% Triton X-100 for 1 hr at 4°C. Cell debris were removed by high-speed centrifugation and the soluble fraction was incubated in the presence of pre-equilibrated amylose resin at 4°C for 1 hour. Following incubation, the resin was washed with lysis buffer, and the fusion protein was eluted with lysis buffer containing 10 mM maltose.

Generation of parasite lines expressing HA-tagged Pfcrk-5

The 3' end of the Pfcrk-5 coding region (856 bp, omitting the stop codon) was amplified by PCR from genomic DNA, using the following primers: Forward: 5'-GGCTGCAGCGTTAATTCTTTAGGTAAACC-3'; Reverse: 5'-CCTGGATCCAAAATGAGAAAATTCTAGATGAC-3', containing *Pst*I and *BamH*1 restriction sites, respectively (underlined), which allowed insertion of the amplified product into pCAM-BSD-HA. Transfection of wild-type 3D7 parasites, selection under blasticidin treatment and dilution cloning were performed as described above for the knock-out parasite line.

Genotype characterisation of Pfcrk-5 gene disruption

PCR: For PCR detection of (i) integration at the 5' and 3' flanks of the insert in the recombined locus, (ii) the wild-type locus and (iii) the episome, various primer combinations were used to amplify PCR products from genomic DNA obtained from transgenic or wild-type parasites. Primer 1: 5'-GGGGGGATCCATGTTTGGAATTACATTAACAAAGTG-3'; primer 2: 5'-TATTCCTAATCATGTAAATCTTAAA-3'; primer 3: 5'-CAATTAACCCTCACTAAAG-3'; primer 4: 5'-CGACCATGTAATTTTACTTCTAC-3'. Primers 1 and 4 hybridise to *pfcrk-5* sequences, while primers 2 and 3 correspond to pCAM-BSD vector sequences flanking the insertion site (see Figures 1 and 3 for primer location).

Southern Blotting: Genomic DNA (gDNA) from wild-type 3D7 and Pfcrk-5 KO parasites was obtained as followed: parasite pellets obtained by saponin lysis were treated with 150 µg/ml Proteinase K and 2% SDS at 55°C for 2 hours. The DNA was precipitated with ethanol and 0.3 M sodium acetate after phenol/chloroform/isoamyl alcohol (25:24:1) extraction. 5 µg of gDNA were then digested with *Nsi*1 or with *Pst*1 and *Swa*1, fractionated on a 0.8 % agarose gel and transferred onto a Hybond N+ membrane. PCR amplicons from either the *pfcrk-5* (the same fragment as that had been inserted into pCAM-BSD, see above) or the *bsd* gene were used as probes, and chemoluminescence detection was performed following the manufacturer's recommendations (Amersham).

Genotype characterisation of Pfcrk-5 HA tagging

PCR: For the detection of integration at the 5' and 3' boundaries of the pCAM-BSD-HA-Pfcrk-5 plasmid, of the episome and of the wild locus, the following primers were used (see Supplementary Figure S3 for primer combinations and locations): Primer 1: 5'-TAACCACAATTGGAGTCGTCG-3'; Primer 2: 5'-TATTCCTAATCATGTAAATCTTAAA-3' ; Primer 3 : 5'-CGAACATTAAGCTGCCATATCC-3' ; Primer 4 : 5'-CAATTAACCCTCACTAAAG-3'; Primer 5: 5'-CAAAAATGTTTTGTTTACATCC-3'.

Southern Blotting: Southern blot was performed as described above, except that genomic DNA extracted from wild-type 3D7 and from Pfcrk-5-HA transgenic parasites was digested with *Cla*1 and *Nco*1.

Anti-Pfcrk-5 antibodies

To obtain chicken IgYs, a peptide (SLGKPNKDELEFFSNSR) was selected from the Pfcrk-5 amino-acid sequence using the Predict7 program, synthesized with an additional C-terminal

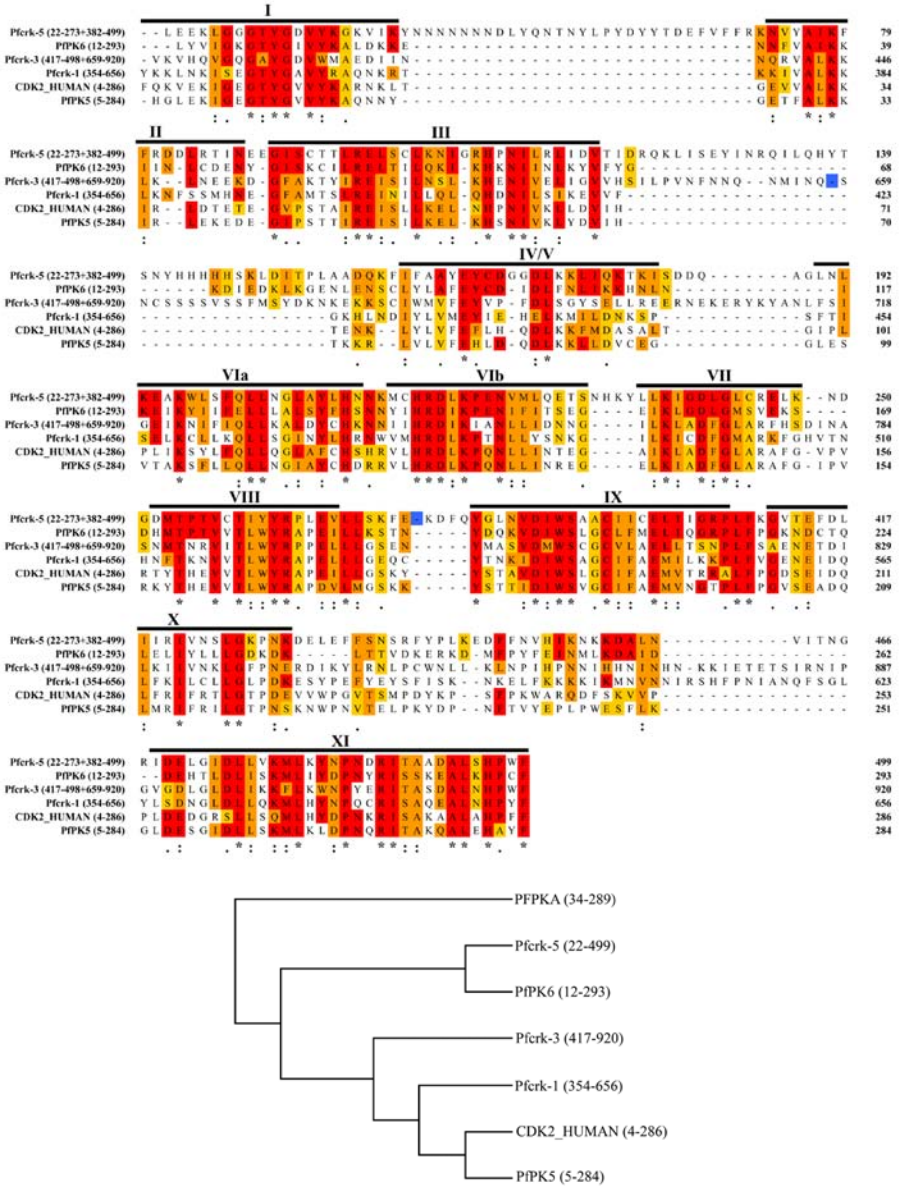

Figure 1. Bioinformatics analyses.
A. Alignment of the Pfcrk-5 kinase domain with that of human CDK2 (CAA43985) and those of other P. falciparum CDK-related sequences: PfPK6 (MAL13P1.185/ PF3D7_1337100), Pfcrk-3 (PFD0740w/ PF3D7_0415300), PfPK5 (MAL13P1.279/ PF3D7_1356900), Pfcrk-1 (PFD0865c/ PF3D7_0417800) was performed with an on-line version of ClustalW2 available on the European Bioinformatics Institute's web site (http://www.ebi.ac.uk/Tools/msa/clustalw2) using default parameters (Protein Weight Matrix: Gonnet, Gap Open cost: 10, Gap Extension: 0.1 for pairwise alignment and 0.2 for multiple sequence alignment). To improve alignment accuracy, large non-conserved regions of the kinase sequences were removed (residues 499 to 658, and 274 to 381 for Pfcrk-3, and Pfcrk-5 respectively). Points of sequence deletion are labelled with a blue (-). Ranges of aligned residues are indicated after each protein name. Colours are used in addition to classical markings to visualize conserved residues: Red/(*) for identity, orange/(:) for strong conservation and yellow/(.) for weak conservation. The 11 subdomains of the kinase catalytic domain are indicated with black bars and roman numbers above the sequences.
B. Cladogram view of a phylogenetic tree built from an equivalent alignment except that the entire kinase domain was used for each protein. Also, the PfPKA kinase domain (PFI1685w/ PF3D7_0934800) was added as an outlier to emphasize the global similarity between the other kinases. The EBI phylogeny tool (http://www.ebi.ac.uk/Tools/phylogeny/clustalw2_phylogeny) was used with default parameters and Unweighted Pair Group Method Arithmetic mean as clustering method.

cysteine (for coupling with MBS), coupled to rabbit albumin carrier and injected into chickens. Anti-peptide antibodies were isolated and affinity purified using the peptide coupled to a Sulpholink (Pierce) affinity matrix as described previously [40].

Rabbit antibodies were produced by Biogene (Germany). Rabbits were immunized with the Pfcrk-5-derived peptide described above for IgY generation, and monospecific rabbit antibodies were immunopurified against the peptide.

Western blotting

Parasites from synchronous cultures were lysed by brief sonication in lysis buffer (50 mM Tris pH 8, 150 mM NaCl,

25 mM $MgCl_2$, 1% Triton, 0.5% NP40, 0.1 mM PMSF, Boehringer protease inhibitors cocktail). The extracts (normalised per protein concentration) were fractionated by SDS-PAGE and blotted onto nitrocellulose. Immunoblotting was carried using a rabbit anti-Pfcrk-5 immunopurified antibody (1/400) and a goat-anti rabbit secondary antibody coupled to peroxidase (1/10000). Immunodetection was performed by chemiluminescence using the ECL system according to the manufacturer's recommended procedure (Amersham). A rabbit anti-Pf Peroxiredoxin antibody (1/4000) was used as a loading control.

Immunoprecipitation

Parasite pellets were sonicated in RIPA buffer (30 mM Tris pH 8.0, 150 mM NaCl, 20 mM $MgCl_2$, 1 mM EDTA, 1 mM dithiothreitol, 10 µM ATP, 0.5% Triton X-100, 1% Nonidet P-40, 10 mM β-glycerophosphate, 10 mM NaF, 0.1 mM sodium orthovanadate, 1 mM phenylmethylsulfonyl fluoride, and Complex™ protease inhibitors). Cold ATP (10 µM) was added to the lysis buffer when immunoprecipitation was to be coupled to a kinase activity assay. The parasite extract (300 µg) was incubated with either immunopurified anti-Pfcrk-5 chicken IgY (4 µg) or with immunopurified anti-Pfcrk-5 rabbit antibody (5 µg) for 2 h at 4°C. The immunocomplexes were precipitated either with 20 µl of a 50% slurry of Protein A-Sepharose CL4B beads coated with anti-chicken IgY rabbit antibodies (Pierce), or with Protein G sepharose beads (Santa Cruz), and washed four times with RIPA buffer. An immunopurified chicken IgY against the human C5a receptor was used as a negative control.

For HA immunoprecipitation, extracts from wild-type 3D7 and from parasites expressing HA-tagged Pfcrk-5 were prepared using the Profound anti-HA Tag IP/Co-IP Kit (Thermoscientific) according to the manufacturer's protocol. 10 µg of mouse anti-HA antibody immobilized on beads (6 µl of beads) were added to both lysates for 2hrs at 4°C. 20 µl of a 50% slurry of Protein G sepharose beads were added prior to washing steps, which were carried out as described above. The immunoprecipitated material was used in kinase assays and/or western blot experiments.

Immunofluorescence assay

IFAs were conducted as described previously [41]. Briefly, cells were fixed in 4% paraformaldehyde/0.075% glutaraldehyde (E.M grade ProSciTech) for 30 minutes at room temperature. Membranes were permeabilised with 0.1% Triton for 10 minutes at room temperature and cells were blocked in 3% BSA-PBS for 1 hour. Cells were incubated successively with primary and secondary antibodies for 1 hour at room temperature. Cells were mounted on a coverslip with Vectashield (Vector laboratories) and DAPI (2 µg/ml). Antibody dilutions were as follow: Rat anti-HA (1/100, Roche), Mouse anti-α-tubulin (1/100, Sigma), Rabbit anti-PK7 (1/150) [42], Rabbit anti-CenPA and Rabbit anti-Nup100 (1/100) [43], Alexa-488, -594 and -647 (1/1000, Molecular Probes). Samples were examined with a DeltaVision Elite deconvolution microscope (Applied Precision). Deconvolution, maximum projection analysis and 3D volume reconstitution were done with Softworx 5.0.0. Fiji and Adobe Photoshop CS5 were used for further image handling.

Kinase assays

The assays were performed in a standard reaction (30 µl) containing 25 mM Tris-HCl pH7.5, 20 mM $MgCl_2$, 2 mM $MnCl_2$, 10 mM NaF, 10 mM β-glycerophosphate, 10 µM ATP, 5 µCi [γ-^{32}P]ATP (6000 Ci/mmol, Perkin Elmer) and 5 µg of Histone H1 (Invitrogen). The kinase reactions were carried out 30 min at 30°C and were stopped by addition of Laemmli buffer, boiled for 3 min and analyzed by electrophoresis on 10% SDS-polyacrylamide gel. The gels were dried and exposed for autoradiography.

Flow cytometry

Highly synchronous parasite culture aliquots (3 µl) were stained with 0.5 µg/mL Acridine Orange (Molecular Probes) in PBS, and the fluorescence profiles of infected erythrocytes were analysed on a BD FACS Canto flow cytometer (BD Biosystems). The cell cycle data were fitted to exponential sine wave equation in GraphPad Prism 5.0.

RESULTS

Bioinformatics

The 705-residue, 82 kDa polypeptide predicted from the single-exon *pfcrk-5* open reading frame contains a predicted kinase catalytic domain (Pfam number PF00069, e-value $1.6e^{-53}$) that possesses all the invariant amino-acids known to be crucial for protein kinase activity (Figure 1A). The Pfcrk-5 catalytic domain carries several insertions located between conserved motifs: a 29-residue insertion between subdomains I and II, a 40-residue insertion between subdomains III and IV (which is the site of similar insertions in the plasmodial CDK-related kinases PfPK6 and Pfcrk-3), an 8-residue insertion between subdomains V and VI (also shared by Pfcrk-3), a short unique 5-residue insertion between subdomains VIb and VII, and finally a unique insertion (111 residues) that is very rich in charged amino acids between subdomains VIII and IX. In addition, it also displays a 206-residue C-terminal extension. Talevich *et al*. identified a novel PTxC motif in the Pfcrk-5 activation loop, which is absent from all CDKs outside Apicomplexa [8]. BLASTP analysis using the Pfcrk-5 sequences as a query retrieved members of the cyclin-dependent kinase family as top scores (not shown). Our initial phylogenetic analysis comprising all plasmodial, yeast and human CMGC kinases [6] suggested that: (i) the closest *P. falciparum* kinase to Pfcrk-5 is PfPK6, a previously described "composite" kinase with similarities to both CDKs and mitogen-activated protein kinases (MAPKs), and whose activity is cyclin-independent [21,26]; and (ii) the Pfcrk-5/PfPK6 branch does not contain orthologues in the yeast or human kinomes. The apicomplexan-specificity of the PfPK6 and Pfcrk-5 orthologous groups was confirmed in the context of an extensive phylogenetic analysis [44]. The phylogenetic analysis presented in Figure 1B confirms the close relatedness between Pfcrk-5 and PfPK6.

Expression of Pfcrk-5 in blood stages

Microarray data available on PlasmoDB [45] show that Pfcrk-5 mRNA is present throughout the erythrocytic asexual cycle, as well as in gametocyte and sporozoites. PCR from genomic DNA and from cDNA libraries from both asexual parasites and gametocytes using primers located at the predicted start and stop codons yielded a 2.1kb amplicon in all cases, indicating that the transcript is not spliced (Figure 2A). Proteomic data available on PlasmoDB detected several Pfcrk-5 peptides in mature gametocytes only; the absence of detection from other stages may reflect low-level expression of the protein. To verify that the enzyme is indeed expressed in asexual parasites, we raised antibodies against a Pfcrk-5-derived peptide and performed western blot analysis of protein extracts from asexual parasites and gametocytes, detecting the expected 82kDa band in both extracts (Figure 2B, lane 1 and 2). This band could be immunoprecipitated from mixed asexual stages with the same antibody (Figure 2C, lane 2), but not with the pre-immune serum (Figure 2C, lane 1). Western blot analysis performed on protein extracts from synchronized cultures of rings, trophozoites and schizonts and using a 2-Cys-peroxiredoxin antibody as a loading control detected Pfcrk-5 mostly in the later stages (Figure 2D), in line with the significantly greater mRNA steady-state levels at this stage (data available on PlasmoDB). A chicken IgY raised against the same Pfcrk-5 peptide gave the same results (Supplementary Figure S1).

Kinase activity of recombinant and native Pfcrk-5

When assayed against histone H1 (a classical CDK substrate), a GST fusion protein comprising the entire coding region of Pfcrk-5 did not display any activity (data not shown). This is to be expected from the fact that Pfcrk-5 belongs to the CDK family, members of which require binding of a cyclin to become active (although it must be noted here that PfPK6, the plasmodial kinase most closely related to Pfcrk-5, does indeed possess cyclin-independent activity [26]). The activity of GST-Pfcrk-5 against histone H1 was then tested in the presence of various recombinant cyclins (Pfcyc-1 [21], Pfcyc-3 [23] , Pfcyc-4 [23] and Ringo [23,46]), and we observed that Pfcyc-1 and Pfcyc-4 were able to activate the kinase (Figure 3A). A kinase-dead mutant (GST-Pfcrk-5/K78M) did not yield any signal in these conditions (Supplementary Figure S2), demonstrating that the activity was indeed due to Pfcrk-5. Immunoprecipitated material obtained from parasite extracts with the anti-Pfcrk-5 antibody possessed strong histone H1 kinase activity, while the controls (immunoprecipitates obtained with pre-immune serum or an irrelevant antibody) did not (Figure 3B). The activity of the native immunoprecipitated was much stronger than that of the recombinant protein, despite much lower amount of the protein in the assay. This presumably reflects that fully activated Pfcrk-5 was immunoprecipitated, while the recombinant protein was not in a fully active configuration, either because the proper cyclin was not present, or because additional activation steps (such

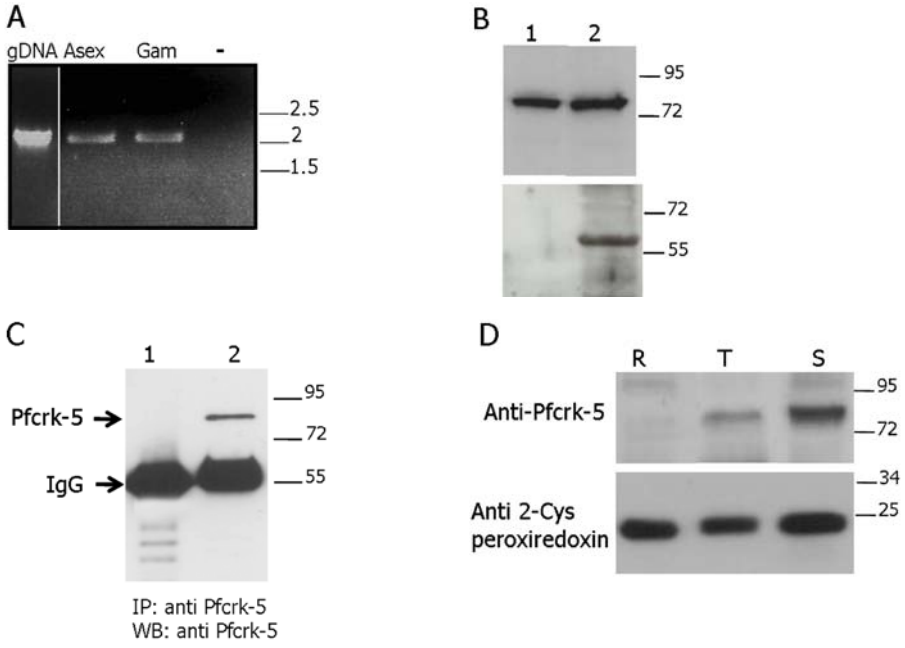

Figure 2. Expression pattern of Pfcrk-5.
A. Amplification of the Pfcrk-5 coding region from 3D7 genomic DNA, and from cDNA libraries from asexual parasites and gametocytes using Pfcrk-5 specific primers. 100 ng of gDNA or cDNA were used. (-) indicates a negative control lane (no DNA or cDNA)
B. Western blot of blood stages using an anti-Pfcrk-5 antibody (upper panel). Lane 1, extract from asexual parasites; lane 2, extract from gametocytes. The lower panel is a loading control (anti-PFA0380w antibody).
C. Western blot of Pfcrk-5 immunoprecipitated from unsynchronised asexual stages. The following antibodies were used for immunoprecipitation: lane 1, pre-immune serum; lane 2, anti-Pfcrk-5 antibody.
D. Western blot of synchronised parasites using an anti-Pfcrk-5 antibody. Extracts were from: R, rings; T, trophozoites and S, schizonts. The lower panel shows an anti-2Cys-peroxiredoxin antibody loading control.

as phosphorylation of a conserved residue in the T-loop) was not achieved in the experiments with recombinant proteins (see Discussion).

C-terminal tagging of the Pfcrk-5 locus

To generate tools for further experiments, we produced transgenic parasite lines expressing HA-epitope-tagged Pfcrk-5 from the cognate locus (see Supplementary Figure S3 for the strategy and genotyping of the clones). A western blot analysis of protein extracts from parental 3D7 and transgenic Pfcrk-5-HA lines, performed using a mouse anti-HA antibody and an anti-PfNapL (PFL0185c) antibody as a loading control, yielded a band at the expected size only in transgenic parasites (Supplementary Figure S4), indicating that the HA-tagged Pfcrk-5 protein is expressed in the transgenic line. As we observed in other cases of locus tagging [34], the wild-type was essentially lost after several months of continuous culture under blasticidin selection. Consistent with data in Figure 3B showing that a Pfcrk-5 antibody can pull down a kinase activity, an immunoprecipitate obtained with the anti-HA antibody from transgenic (but not from wild-type) parasites contained strong histone H1 kinase activity (Figure 3C). Immunofluorescence microscopy of the transgenic line using the anti-HA antibody yielded a weak signal in rings and trophozoites (not shown) and a more intense signal in schizonts (Figure 4); no HA signal was detected in wild-type parasites (Figure 4E). At all stages Pfcrk-5-HA presents a dot-like pattern, with signal intensity increasing with parasite maturation. Pfcrk-5 clearly resides in the nuclear periphery, as evidenced by the observation that Pfcrk-5 dots are always within the boundaries defined by the CenPA and Nup100 markers of nuclear periphery (Supplemental Figure S5 and Movies S5A and S5B), although strict co-localisation with these proteins was not observed (Figure 4A and 4B). Furthermore, Pfcrk-5 does not associate with microtubules as show by the absence of co-localisation with α-tubulin (Figure 4C). Information on the Pfcrk-5 expression profile derived from IFA is fully consistent with microarrays, proteomics and western blot data (Figure 2) showing highest level of this CDK in mature asexual stages.

A functional pfcrk-5 gene is not required for asexual growth

We transfected 3D7 parasites with a construct aimed at disrupting the *pfcrk-5* locus, following a strategy that has been described in detail elsewhere ([47]; see Supplemental Figure S6 for details on the knock-out strategy and genotyping of the knock-out clones). Briefly, homologous recombination of the plasmid into the *pfcrk-5* locus is expected to result in a pseudo-diploid configuration, with both truncated copies lacking essential residues. After two independent transfections, the *pfcrk-5* locus of blasticidin-resistant parasites was examined by PCR, which clearly demonstrated that the plasmid had integrated into the locus (Figure S6B, left panel; a succinct report of these experiments can be found in our recent report describing the kinome-wide reverse genetics approach [27]). We proceeded with obtaining individual clones from both independently transfected

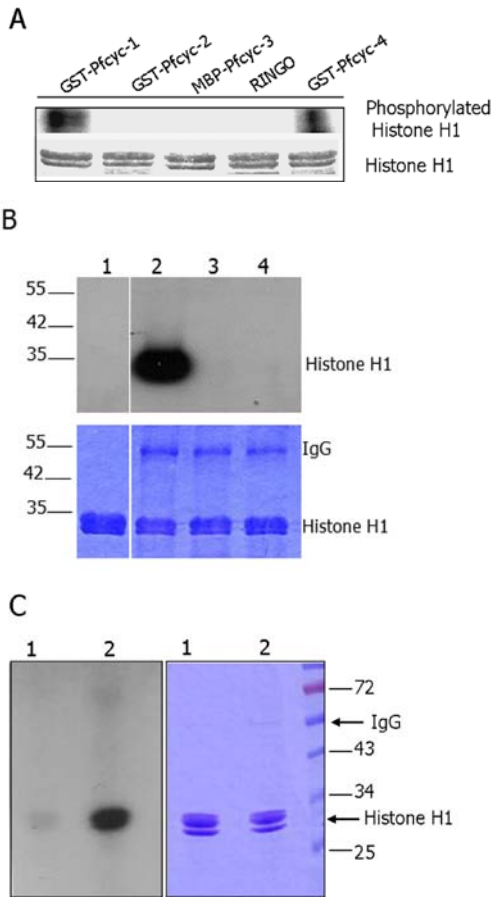

Figure 3. Kinase activity of recombinant and native Pfcrk-5.
A. Kinase assays using recombinant proteins. In vitro kinase assays were performed using 0.5 µg of recombinant GST-Pfcrk-5 and Histone H1 as a substrate with the following cyclin partners (0.5 µg to 1 µg): lane 2, GST-Pfcyc-2; lane 3, MBP-Pfcyc-3; lane 4, MBP-Ringo; lane 5, GST-Pfcyc-4. Top panel: autoradiogram following kinase reaction; bottom panel: Coomassie-stained gel. Pfcrk-5 phosphorylates Histone H1 in the presence of Pfcyc-1 and Pfcyc-4, but not in the presence of the other cyclins.
B. Kinase activity of native Pfcrk-5 immunoprecipitated from wild-type parasite extracts. An immunopurified chicken anti-Pfcrk-5 IgY was incubated with a schizont protein extract (lane 2). The immunocomplexes were pelleted with protein A-agarose beads and subjected to a kinase assay using Histone H1 as an exogenous substrate. A control reaction with the substrate alone was included (lane 1). Additional negative controls consisted of an immunoprecipitation with the same antibody from lysis buffer only (no parasite material) (lane 3) or with an irrelevant immunopurified IgY (against the human C5 receptor) (lane 4). The top panel shows the autoradiogramme, the bottom panel shows a Coomassie stain of the gel.
C. Kinase activity of HA-tagged Pfcrk-5 immunoprecipitated from transgenic parasite extracts using an anti-HA antibody. Lane 1, immunoprecipitation from an extract from wild-type 3D7; lane 2, immunoprecipitation form an extract from transgenic parasites with an HA-tagged pfcrk-5 locus. The left panel shows the autoradiogramme, the right panel shows a Coomassie stain of the gel.

populations by limiting dilution, and clones from each population (clones A3 and C1) were genotyped by PCR and Southern blot (Figure S6B and S6C respectively). No wild-type locus bands were detected with either method, whereas bands that are

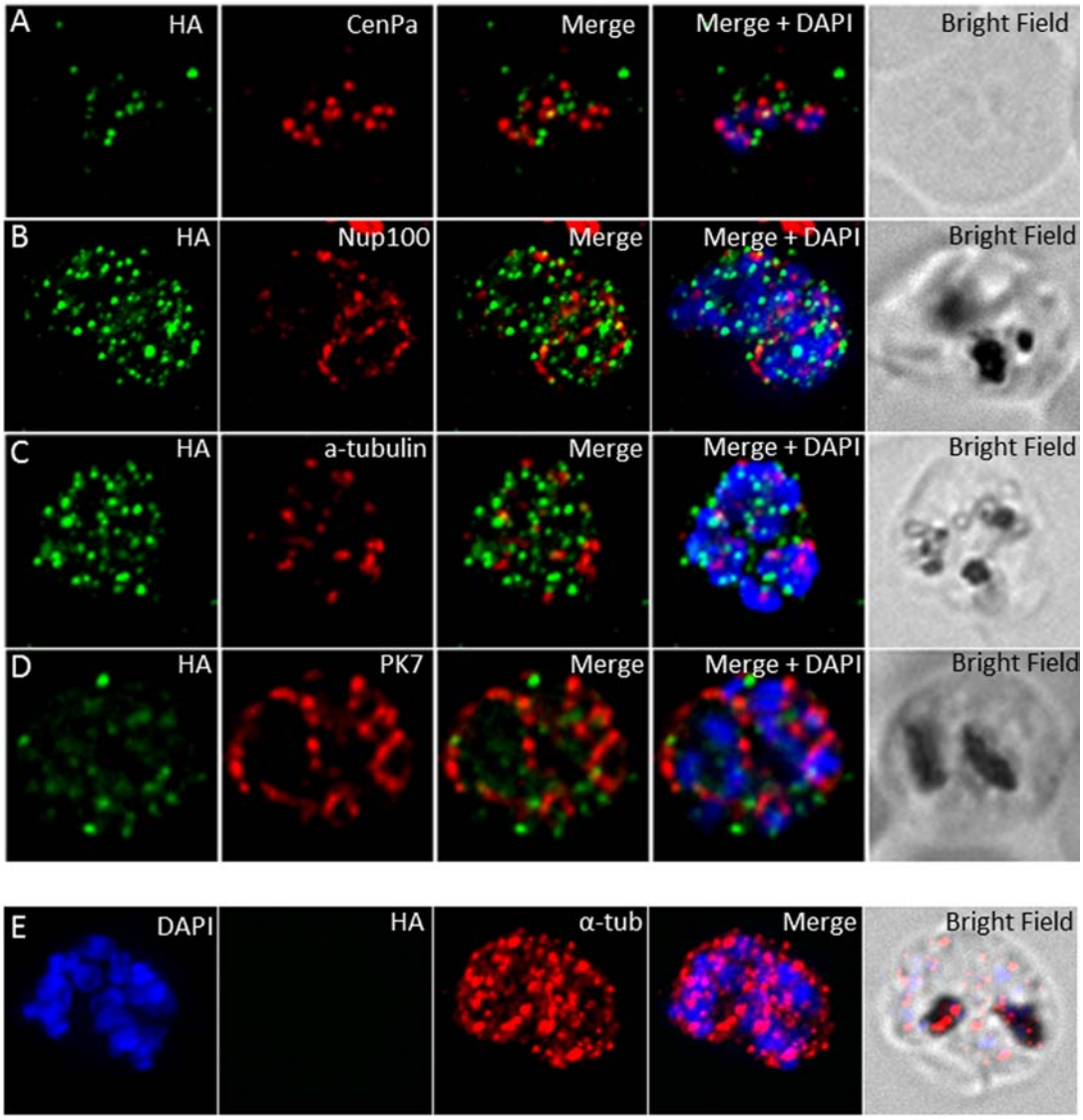

Figure 4. Detection of HA-Pfcrk-5 by immunofluorescence microscopy. IFAs of asynchronous asexual transgenic Pfcrk-5-HA (A – D) and wild-type 3D7 (E) parasites. A. anti-HA and anti-CenPA. B. anti-HA and anti-Nup100. C. anti-HA and anti-α-tubulin. D. anti-HA and anti-PK7. E. anti-HA and anti-α-tubulin.

diagnostic for locus disruption were very clear in both clones. We verified the absence of the Pfrck-5 protein in the *pfcrk-5*$^{-}$ clones by western blot. Figure 5A shows the data for clone C1; the same was observed with clone A3, using a chicken IgY (data not shown); consistently, no kinase activity was pulled-downed with the anti-Pfcrk-5 antibody from the *pfcrk-5*$^{-}$ parasites (Figure 5B). These experiments, in addition to validating the KO clones as unable to express Pfcrk-5 to a detectable level, also provide an excellent control for the experiments in Figure 3.

Proliferation rate phenotype of pfcrk-5^{-} clones.

Our success in obtaining *pfcrk-5*$^{-}$ parasites strongly suggested that parasites are viable in the absence of a *pfcrk-5* gene, and hence that the enzyme is dispensable for completion of the erythrocytic asexual cycle. However, by monitoring the growth rate of both KO clones in comparison to that of the 3D7 parental clone, we initially observed that the parasitemia growth rate was impaired in the *pfcrk-5*$^{-}$ parasites [27]. This study was repeated (Figure 6A) and extended by investigations into the mechanism underpinning the slow growth rate. In particular, we were intrigued by the similarity in the wild-type/KO growth rate ratios for *pfcrk-5*$^{-}$ parasites (this study) and for parasite clones lacking another kinase, PfPK7, which also increased their parasitemia at approximately half the rate of wild-type parasites [28]. The slow growth of *PfPK7*$^{-}$ parasites is caused by a decrease in the number of merozoites generated per segmenter [28]. Microscopic observation of segmenters from parental and *pfcrk-5*$^{-}$ parasites pointed to a decrease in the number of nuclei per schizont in the KO clones, suggesting that a smaller progeny underpins the growth phenotype for these parasites,

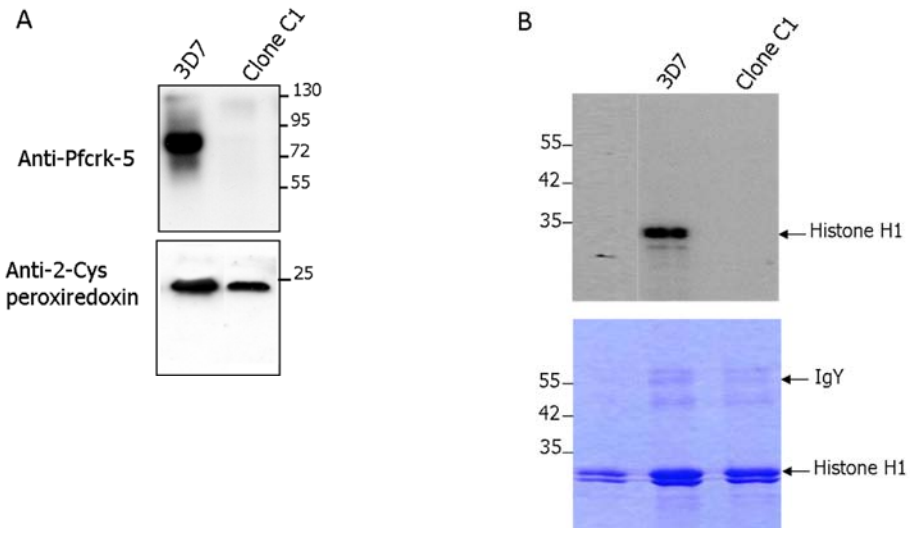

Figure 5. *Pfcrk-5 expression and kinase activity in wild-type and pfcrk-5⁻ parasites.*
A. Western blot analysis. Top panel: Protein extracts (15 μg) from wild-type 3D7 (lane 1) and pfcrk-5⁻ schizonts clone C1 (lane 2) were fractionated by SDS-PAGE, transferred and probed with an anti-Pfcrk-5 antibody. An anti-2Cys-peroxyredoxin antibody was used as a loading control (bottom panel). The sizes of co-migrating markers are indicated in kDa.
B. Immunoprecipitated kinase activity. An immunopurified chicken anti-Pfcrk-5 IgY was incubated with extracts from wild-type 3D7 or from pfcrk-5⁻ parasites (clone C1). Immuno-complexes were recovered and subjected to a kinase reaction as described in the legend to Figure 3.

as demonstrated for *pfpk7*⁻ parasites (Figure 6B). To formally validate this observation, flow cytometry analysis based on DNA content [48] was applied to the mutant clones and parental wild-type 3D7, which showed that the proportion of schizonts with >16N DNA was considerably lower in the *pfcrk-5*⁻ clones than in wild-type parasites (Figure 6C). Furthermore, measuring fluctuations of the percentage of parasites with >16N over two life cycles confirmed the lower proportion of parasites with many genomes, and, in addition, did not detect any significant difference in the length of the life cycle between wild-type and *pfcrk-5*⁻ parasites (Figure 6D). Pfcrk-5 disruption does not seem to alter gametocytogenesis, as the morphology of *pfcrk-5*⁻ male and female gametocytes did not display any obvious defect under admittedly superficial Giemsa-based microscopic examination (data not shown). The very close similarity between the PfPK7 [27] and Pfcrk-5 KO phenotypes raises the possibility that these two enzymes function in the same pathway. Although both kinases localize to the nuclear periphery, no co-localization was observed (Figure 4D) (see Discussion).

DISCUSSION

Cell cycle control in malaria parasites is far from being understood. One approach to fill this important gap in our knowledge of *Plasmodium* basic biology is to characterize the function of regulatory enzymes, which, by analogy with their known functions in other eukaryotes, are putative cell cycle control elements. This is the case for the *P. falciparum* CDK-related enzymes. Here we functionally characterize Pfcrk-5, the last of the six CDK-like enzymes encoded in the parasite's genome to be investigated at the biochemical level. Its phylogenetic isolation from "classical" mammalian and yeast CDKs (it does not cluster with any of the enzymes in these systems [6,8] and is part of an orthologous group that is specific to Apicomplexa [44]) make it impossible to predict precise cellular functions for Pfcrk-5. We show here that Pfcrk-5 is part of a regulatory pathway that controls the number of merozoites in schizont progeny, as *pfcrk-5*⁻ schizonts produce fewer nuclear bodies (and hence, most presumably fewer daughter merozoites) than wild-type parasites. This is strikingly similar to the phenotype that we reported earlier for PfPK7, an "orphan" kinase that has no orthologues outside Apicomplexa. That both Pfcrk-5 and PfPK7 are enzymes found only in apicomplexan parasites is consistent with their involvement in a cellular process (schizogony) that is not shared by yeast or mammalian cells.

Pfcrk-5 clearly clusters within the CDK family, but forms a distinct branch therein that also contains PfPK6, a cyclin-independent enzyme thought to be involved in the onset of S-phase in the trophozoite [26], but no human or yeast sequences [6]. Here we show that in contrast Pfcrk-5 does require cyclin binding to become active. We were not able to predict this on the basis of the cyclin-binding motif, which is PSTAIRE in CDK2 and is substituted by SCTTLRE in Pfcrk-5 and SKCILRE in PfPK6. Two of the four identified *P. falciparum* cyclins are able to activate recombinant Pfcrk-5 *in vitro*. However, the specific activity in these conditions is much smaller than that observed with Pfcrk-5 obtained by immunoprecipitation from parasite extracts. This most likely reflects the fact that a full activity is not obtained with the recombinant CDK/cyclin complex. It is well established that cyclin binding only partially activates canonical CDKs such as human CDK2. Cyclin binding renders a conserved threonine residue (Thr 160 in CDK2) in the activation loop accessible to phosphorylation by the CAK, which fully activates the enzyme [49]. The phosphothreonine acts as an organizing center that establishes electreostatic interactions with three

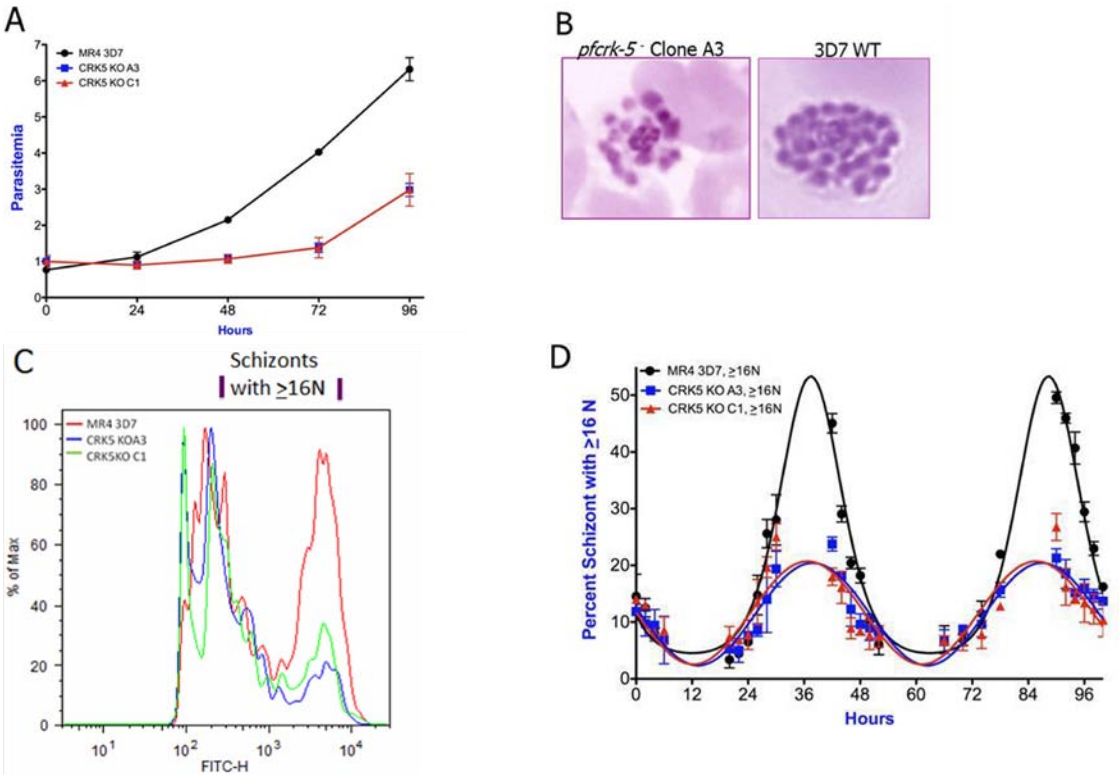

Figure 6. *Phenotype analysis of pfcrk-5⁻ parasites.*
A. Growth curve of wild-type 3D7 and of pfcrk-5⁻ clones: Parasitemia of synchronous cultures were measured every 24 hrs by flow cytometry and average parasitemia is plotted against time for wild-type (circles) and knockout clone A3 (squares) and clone C1 (triangles). Error bars indicate the standard deviation of triplicate samples.
B. Phenotype of schizonts: Giemsa-stained smear of schizont-stage parasites from wild-type culture and knockout clone A3. The "fewer merozoites per schizont" phenotype in the pfcrk-5⁻ culture (versus wild-type 3D7) was observed in > 10 different fields of Giemsa-stained smears.
C. DNA content of schizont stage parasites: fluorescence profiles of infected erythrocytes by flow cytometry analysis are shown. The fluorescence peak of wild-type 3D7 is much higher than that of knockout clones A3 and C1.
D. Parasite cycle time of wild-type and knockout clones: Parasitemia of highly synchronous cultures were measured by flow cytometry every 2 to 3 hrs over two cycles. Out of the total parasitemia, the schizont stage population was selected and plotted as percent schizont with > 16N over time. The data were fit to an exponential sine wave equation and the resulting curves are shown with error bars indicating the standard deviation of triplicate samples. No difference in periodicity was observed between wild-type 3D7 and knockout clones.

neighboring arginine residues (Arg50, Arg126 and Arg150), stabilizing the active, extended conformation of the T-loop [50]. The threonine and all three arginine residues are present in Pfcrk-5 (Figure 1A), suggesting this activation mechanism may be conserved. Although Pfcyc-1 and Pfcyc-4 are able to activate Pfcrk-5 to some extent *in vitro*, in the absence of any information to demonstrate that Pfcrk-5 forms complexes with cyclins within parasites, the physiological relevance of these observations remains uncertain. Furthermore, we cannot exclude that the *in vivo* activator is different from Pfcyc-1/Pfcyc-4, as the four cyclin-like proteins identified in *P. falciparum* may not be the only CDK activators encoded in the *P. falciparum* genome: non-cyclin CDK activators do actually exist in eukaryotic systems [51], and one can speculate that some of the "hypothetical proteins" that make up more than half the parasite's proteome might have such a function. The cognate cyclin(s) and other regulatory proteins might be identified through an interactomics approach. We attempted to purify Pfcrk-5-containing complexes by immunoprecipitation of the HA-tagged enzymes from transgenic parasites using an anti-HA antibody, but so far we have been unsuccessful in our attempts to identify co-precipitating proteins by mass spectrometry, presumably because of the low abundance of the enzyme (this approach generated useful results when applied to a more abundant protein kinase, PfCK2 [52]). We are attempting scaling up the process for Pfcrk-5, as identifying interactors would provide useful insight not only about the cyclin(s) and other regulators of Pfcrk-5 activity, but also into the effectors of the enzyme's action on nuclear division control. In view of the close similarity between the PfPK7 and Pfcrk-5 knock-out phenotypes, it would be of particular interest to determine whether the two enzymes interact with each other. Although no *in vivo* co-localisation of Pfcrk-5 and PfPK7 was observed in schizonts (Figure 4D), we cannot exclude a transient interaction between these two kinases at a specific point in the nuclear division cycle. Our preliminary results using recombinant proteins (data not shown) indicate that His-tagged PfPK7 (but not another His-tagged kinase used as a control) can be pulled-down *via* GST-tagged Pfcrk-5 using glutathione beads, and, vice-versa, that GST-tagged Pfcrk-5 (but not another GST-tagged kinase) can be pulled via His-tagged PfPK7 using nickel

beads; the possible *in vivo* relevance of this observation remains to be established.

Parasites lacking PfPK7 not only have a reduced proliferation rate during erythrocytic schizogony, but also are unable to develop from ookinete to oocyst in the mosquito vector [28]. Since the generation of sporozoites in the oocyst also represents a case of asexual proliferation (like erythrocytic schizogony), the molecular basis for both phenotypes might be similar. It would be of great interest to investigate the fate of *pfcrk-5*$^{-}$ parasites in the mosquito. The hypothesis they would display a similar oocyst phenotype to that of the PfPK7 knock-out is testable, since the lack of Pfcrk-5 does not interfere with the formation of mature gametocytes.

Acknowledgments

This research received funding from the European Community's Seventh Framework Programme (FP7/2007-2013) (MALSIG project to CD and SD) and EviMalar network of Excellence to CD), the FP6 (SIGMAL and ANTIMAL projects to CD), and received additional support from Inserm, EPFL, and Monash University.

Conflict of interest

The authors have no conflict of interest to mention.

References

[1] Dondorp, A.M., S. Yeung, L. White, C. Nguon, N.P. Day, D. Socheat, and L. von Seidlein, Artemisinin resistance: current status and scenarios for containment. Nat Rev Microbiol, 2010. 8(4): p. 272-80.

[2] Wells, T.N. and E.M. Poll, When is enough enough? The need for a robust pipeline of high-quality antimalarials. Discov Med, 2010. 9(48): p. 389-98.

[3] Zhang, J., P.L. Yang, and N.S. Gray, Targeting cancer with small molecule kinase inhibitors. Nat Rev Cancer, 2009. 9(1): p. 28-39.

[4] Doerig, C. and L. Meijer, Antimalarial drug discovery: targeting protein kinases. Expert Opin Ther Targets, 2007. 11(3): p. 279-90.

[5] Jirage, D., S.M. Keenan, and N.C. Waters, Exploring novel targets for antimalarial drug discovery: plasmodial protein kinases. Infect Disord Drug Targets, 2010. 10(3): p. 134-46.

[6] Ward, P., L. Equinet, J. Packer, and C. Doerig, Protein kinases of the human malaria parasite Plasmodium falciparum: the kinome of a divergent eukaryote. BMC Genomics, 2004. 5: p. 79.

[7] Anamika, N. Srinivasan, and A. Krupa, A genomic perspective of protein kinases in Plasmodium falciparum. Proteins, 2005. 58(1): p. 180-9.

[8] Talevich, E., A. Mirza, and N. Kannan, Structural and evolutionary divergence of eukaryotic protein kinases in Apicomplexa. BMC evolutionary biology, 2011. 11(1): p. 321-321.

[9] Schneider, A.G. and O. Mercereau-Puijalon, A new Apicomplexa-specific protein kinase family: multiple members in Plasmodium falciparum, all with an export signature. BMC Genomics, 2005. 6: p. 30.

[10] Satyanarayana, A. and P. Kaldis, Mammalian cell-cycle regulation: several Cdks, numerous cyclins and diverse compensatory mechanisms. Oncogene, 2009. 28(33): p. 2925-39.

[11] Galons, H., N. Oumata, and L. Meijer, Cyclin-dependent kinase inhibitors: a survey of recent patent literature. Expert Opin Ther Pat, 2010. 20(3): p. 377-404.

[12] Cicenas, J. and M. Valius, The CDK inhibitors in cancer research and therapy. J Cancer Res Clin Oncol, 2011. 137(10): p. 1409-18.

[13] Krystof, V. and S. Uldrijan, Cyclin-dependent kinase inhibitors as anticancer drugs. Curr Drug Targets, 2010. 11(3): p. 291-302.

[14] Zhu, J., W. Li, and Z. Mao, Cdk5: mediator of neuronal development, death and the response to DNA damage. Mech Ageing Dev, 2011. 132(8-9): p. 389-94.

[15] Garriga, J. and X. Grana, Cellular control of gene expression by T-type cyclin/CDK9 complexes. Gene, 2004. 337: p. 15-23.

[16] Akoulitchev, S., S. Chuikov, and D. Reinberg, TFIIH is negatively regulated by cdk8-containing mediator complexes. Nature, 2000. 407(6800): p. 102-6.

[17] Kasten, M. and A. Giordano, Cdk10, a Cdc2-related kinase, associates with the Ets2 transcription factor and modulates its transactivation activity. Oncogene, 2001. 20(15): p. 1832-8.

[18] Loyer, P., J.H. Trembley, R. Katona, V.J. Kidd, and J.M. Lahti, Role of CDK/cyclin complexes in transcription and RNA splicing. Cell Signal, 2005. 17(9): p. 1033-51.

[19] Fisher, R.P., Secrets of a double agent: CDK7 in cell-cycle control and transcription. J Cell Sci, 2005. 118(Pt 22): p. 5171-80.

[20] Doerig, C.D., Stopping malaria parasites dead in their tracks. Nat Chem Biol, 2008. 4(6): p. 334-5.

[21] Le Roch, K., C. Sestier, D. Dorin, N. Waters, B. Kappes, D. Chakrabarti, L. Meijer, and C. Doerig, Activation of a Plasmodium falciparum cdc2-related kinase by heterologous p25 and cyclin H. Functional characterization of a P. falciparum cyclin homologue. J Biol Chem, 2000. 275(12): p. 8952-8.

[22] Waters, N.C., C.L. Woodard, and S.T. Prigge, Cyclin H activation and drug susceptibility of the Pfmrk cyclin dependent protein kinase from Plasmodium falciparum. Mol Biochem Parasitol, 2000. 107(1): p. 45-55.

[23] Merckx, A., K. Le Roch, M.P. Nivez, D. Dorin, P. Alano, G.J. Gutierrez, A.R. Nebreda, D. Goldring, C. Whittle, S.

Patterson, D. Chakrabarti, and C. Doerig, Identification and initial characterization of three novel cyclin-related proteins of the human malaria parasite Plasmodium falciparum. J Biol Chem, 2003. 278(41): p. 39839-50.

[24] Halbert, J., L. Ayong, L. Equinet, K. Le Roch, M. Hardy, D. Goldring, L. Reininger, N. Waters, D. Chakrabarti, and C. Doerig, A Plasmodium falciparum transcriptional cyclin-dependent kinase-related kinase with a crucial role in parasite proliferation associates with histone deacetylase activity. Eukaryot Cell, 2010. 9(6): p. 952-9.

[25] Li, J.L., K.J. Robson, J.L. Chen, G.A. Targett, and D.A. Baker, Pfmrk, a MO15-related protein kinase from Plasmodium falciparum. Gene cloning, sequence, stage-specific expression and chromosome localization. Eur J Biochem, 1996. 241(3): p. 805-13.

[26] Bracchi-Ricard, V., S. Barik, C. Delvecchio, C. Doerig, R. Chakrabarti, and D. Chakrabarti, PfPK6, a novel cyclin-dependent kinase/mitogen-activated protein kinase-related protein kinase from Plasmodium falciparum. Biochem J, 2000. 347 Pt 1: p. 255-63.

[27] Solyakov, L., J. Halbert, M.M. Alam, J.P. Semblat, D. Dorin-Semblat, L. Reininger, A.R. Bottrill, S. Mistry, A. Abdi, C. Fennell, Z. Holland, C. Demarta, Y. Bouza, A. Sicard, M.P. Nivez, S. Eschenlauer, T. Lama, D.C. Thomas, P. Sharma, S. Agarwal, S. Kern, G. Pradel, M. Graciotti, A.B. Tobin, and C. Doerig, Global kinomic and phospho-proteomic analyses of the human malaria parasite Plasmodium falciparum. Nat Commun, 2011. 2: p. 565.

[28] Dorin-Semblat, D., A. Sicard, C. Doerig, and L. Ranford-Cartwright, Disruption of the PfPK7 gene impairs schizogony and sporogony in the human malaria parasite Plasmodium falciparum. Eukaryot Cell, 2008. 7(2): p. 279-85.

[29] Leete, T.H. and H. Rubin, Malaria and the cell cycle. Parasitol Today, 1996. 12(11): p. 442-4.

[30] Arnot, D.E. and K. Gull, The Plasmodium cell-cycle: facts and questions. Ann Trop Med Parasitol, 1998. 92(4): p. 361-5.

[31] Arnot, D.E., E. Ronander, and D.C. Bengtsson, The progression of the intra-erythrocytic cell cycle of Plasmodium falciparum and the role of the centriolar plaques in asynchronous mitotic division during schizogony. Int J Parasitol, 2011. 41(1): p. 71-80.

[32] Read, M., T. Sherwin, S.P. Holloway, K. Gull, and J.E. Hyde, Microtubular organization visualized by immunofluorescence microscopy during erythrocytic schizogony in Plasmodium falciparum and investigation of post-translational modifications of parasite tubulin. Parasitology, 1993. 106 (Pt 3): p. 223-32.

[33] Reininger, L., J.M. Wilkes, H. Bourgade, D. Miranda-Saavedra, and C. Doerig, An essential Aurora-related kinase transiently associates with spindle pole bodies during Plasmodium falciparum erythrocytic schizogony. Mol Microbiol, 2011. 79(1): p. 205-21.

[34] Dorin-Semblat, D., N. Quashie, J. Halbert, A. Sicard, C. Doerig, E. Peat, and L. Ranford-Cartwright, Functional characterization of both MAP kinases of the human malaria parasite Plasmodium falciparum by reverse genetics. Mol Microbiol, 2007. 65(5): p. 1170-80.

[35] Lambros, C. and J.P. Vanderberg, Synchronization of Plasmodium falciparum erythrocytic stages in culture. J Parasitol, 1979. 65(3): p. 418-20.

[36] Carter, R., L. Ranford-Cartwright, and P. Alano, The culture and preparation of gametocytes of Plasmodium falciparum for immunochemical, molecular, and mosquito infectivity studies. Methods Mol Biol, 1993. 21: p. 67-88.

[37] Ho, S.N., H.D. Hunt, R.M. Horton, J.K. Pullen, and L.R. Pease, Site-directed mutagenesis by overlap extension using the polymerase chain reaction. Gene, 1989. 77(1): p. 51-9.

[38] Sidhu, A.B., S.G. Valderramos, and D.A. Fidock, pfmdr1 mutations contribute to quinine resistance and enhance mefloquine and artemisinin sensitivity in Plasmodium falciparum. Mol Microbiol, 2005. 57(4): p. 913-26.

[39] Rosario, V., Cloning of naturally occurring mixed infections of malaria parasites. Science, 1981. 212(4498): p. 1037-8.

[40] Hurdayal, R., I. Achilonu, D. Choveaux, T.H. Coetzer, and J.P. Dean Goldring, Anti-peptide antibodies differentiate between plasmodial lactate dehydrogenases. Peptides, 2010. 31(4): p. 525-32.

[41] Tonkin, C.J., G.G. van Dooren, T.P. Spurck, N.S. Struck, R.T. Good, E. Handman, A.F. Cowman, and G.I. McFadden, Localization of organellar proteins in Plasmodium falciparum using a novel set of transfection vectors and a new immunofluorescence fixation method. Mol Biochem Parasitol, 2004. 137(1): p. 13-21.

[42] Dorin, D., J.P. Semblat, P. Poullet, P. Alano, J.P. Goldring, C. Whittle, S. Patterson, D. Chakrabarti, and C. Doerig, PfPK7, an atypical MEK-related protein kinase, reflects the absence of classical three-component MAPK pathways in the human malaria parasite Plasmodium falciparum. Mol Microbiol, 2005. 55(1): p. 184-96.

[43] Volz, J., T.G. Carvalho, S.A. Ralph, P. Gilson, J. Thompson, C.J. Tonkin, C. Langer, B.S. Crabb, and A.F. Cowman, Potential epigenetic regulatory proteins localise to distinct nuclear sub-compartments in Plasmodium falciparum. Int J Parasitol. 40(1): p. 109-21.

[44] Miranda-Saavedra, D., T. Gabaldon, G.J. Barton, G. Langsley, and C. Doerig, The kinomes of apicomplexan parasites. Microbes Infect, 2012. 14(10): p. 796-810.

[45] Le Roch, K.G., Y. Zhou, P.L. Blair, M. Grainger, J.K. Moch, J.D. Haynes, P. De La Vega, A.A. Holder, S. Batalov, D.J. Carucci, and E.A. Winzeler, Discovery of gene function by expression profiling of the malaria parasite life cycle. Science, 2003. 301(5639): p. 1503-8.

[46] Ferby, I., M. Blazquez, A. Palmer, R. Eritja, and A.R. Nebreda, A novel p34(cdc2)-binding and activating protein that is necessary and sufficient to trigger G(2)/M progression in Xenopus oocytes. Genes Dev, 1999. 13(16): p. 2177-89.

[47] Doerig, C., A. Abdi, N. Bland, S. Eschenlauer, D. Dorin-Semblat, C. Fennell, J. Halbert, Z. Holland, M.P. Nivez, J.P.

Semblat, A. Sicard, and L. Reininger, Malaria: targeting parasite and host cell kinomes. Biochim Biophys Acta, 2010. 1804(3): p. 604-12.

[48] Liu, J., I.Y. Gluzman, M.E. Drew, and D.E. Goldberg, The role of Plasmodium falciparum food vacuole plasmepsins. J Biol Chem, 2005. 280(2): p. 1432-7.

[49] Otyepka, M., I. Bartova, Z. Kriz, and J. Koca, Different mechanisms of CDK5 and CDK2 activation as revealed by CDK5/p25 and CDK2/cyclin A dynamics. J Biol Chem, 2006. 281(11): p. 7271-81.

[50] Russo, A.A., P.D. Jeffrey, and N.P. Pavletich, Structural basis of cyclin-dependent kinase activation by phosphorylation. Nat Struct Biol, 1996. 3(8): p. 696-700.

[51] Nebreda, A.R., CDK activation by non-cyclin proteins. Curr Opin Cell Biol, 2006. 18(2): p. 192-8.

[52] Dastidar, E.G., G. Dayer, Z.M. Holland, D. Dorin-Semblat, A. Claes, A. Chene, A. Sharma, R. Hamelin, M. Moniatte, J.J. Lopez-Rubio, A. Scherf, and C. Doerig, Involvement of Plasmodium falciparum protein kinase CK2 in the chromatin assembly pathway. BMC Biol, 2012. 10(1): p. 5.